

引用格式:焦智,丁文宇,杨富强,等.能谱CT材料分解算法研究进展[J].材料工程,2025,53(11):30-48.
JIAO Zhi,DING Wenyu,YANG Fuqiang, et al.Research progress in material decomposition algorithms for spectral CT[J].
Journal of Materials Engineering,2025,53(11):30-48.

能谱 CT 材料分解算法研究进展

Research progress in material decomposition algorithms for spectral CT

焦 智^{1,2},丁文宇³,杨富强^{1,2},黄魁东^{1,2*}

(1 西北工业大学 机电学院,西安 710072;2 西北工业大学
宁波研究院,浙江 宁波 315000;3 陕西应用物理化学
研究所,西安 710061)

JIAO Zhi^{1,2},DING Wenyu³,YANG Fuqiang^{1,2},
HUANG Kuidong^{1,2*}

(1 School of Mechanical and Electrical Engineering, Northwestern
Polytechnical University, Xi'an 710072, China; 2 Ningbo
Research Institute, Northwestern Polytechnical University,
Ningbo 315000, Zhejiang, China; 3 Shaanxi Institute of
Applied Physics and Chemistry, Xi'an 710061, China)

摘要:能谱计算机层析成像(spectral computed tomography, spectral CT)是一种新兴的检测技术,它通过测量物体对不同能量X射线的吸收情况,可以获得更丰富的组织成分信息,在医疗诊断、无损检测、材料分析、安全监测等多个领域发挥着重要作用。材料分解算法是能谱CT技术的核心,旨在从多能量数据中分解出不同组织的成分信息,是提升分解图像质量和准确性的关键。本文综述了能谱CT的数据采集方式和材料分解数学模型,重点梳理讨论了能谱CT材料分解算法在投影域、图像域、直接迭代和基于深度学习4个方面的研究进展,深入比较分析了各类算法的理论优势、技术限制以及当前的应用情况,指出了投影域的混合分解优化、图像域的融合先验约束和多模态数据、直接迭代的收敛稳定性改进、深度学习的迁移和高泛化性是本领域未来研究工作的发展趋势。

关键词:能谱CT;材料分解;无损检测;深度学习

doi: 10.11868/j.issn.1001-4381.2025.000126 **CSTR:** 32421.14.j.issn.1001-4381.2025.000126

中图分类号: TP391.4;TH74 **文献标识码:** A **文章编号:** 1001-4381(2025)11-0030-19

Abstract: Spectral computed tomography (spectral CT) is an emerging detection technology that acquires more comprehensive tissue composition information by measuring an object's absorption of X-rays of different energies. It plays a pivotal role in various fields such as medical diagnosis, non-destructive testing, material analysis, and security monitoring. Material decomposition algorithms are the core of spectral CT technology, aiming to decompose the composition information of different tissues from multi-energy data. These algorithms are crucial for enhancing the quality and accuracy of decomposed images. This paper reviews the data acquisition methods and mathematical models for material decomposition in spectral CT. It focuses on discussing the research progress of spectral CT material decomposition algorithms in four aspects: projection domain, image domain, direct iteration, and deep learning-based methods. It conducts an in-depth comparative analysis of the theoretical advantages, technical limitations, and current application status of various algorithms. The paper points out that the future research trends in this field include hybrid decomposition optimization in the projection domain, fusion prior constraints and multi-model data in the image domain, convergence stability improvements in direct iteration, and transferability and high generalization in deep learning.

Key words: spectral CT; material decomposition; non destructive testing; deep learning

计算机层析成像(computed tomography, CT)作为 1 种重要的检测技术,它能够无损、非接触地获取物体内部物质和结构信息^[1-2]。然而,传统的 CT 成像技术只能提供关于物体的形态和密度信息,对于物体的组织成分识别和定量化分析的需求无法满足^[3]。为了克服此限制,能谱计算机层析成像(spectral computed tomography, spectral CT)技术应运而生,通过获取 X 射线在不同能量范围内的衰减信息,能够提供更丰富的组织成分和材料信息,为相关技术的拓展和性能突破提供了更多的可能性^[4-5]。能谱 CT 的应用范围广泛,涵盖了医疗诊断^[6-7]、无损检测^[8-9]、材料分析^[10-11]、安全监测^[12-13]等领域,对于实现精确的组织分割、病变检测、缺陷检测和材质识别具有重要意义。

在能谱 CT 中,材料分解算法是实现对物体成分准确识别和定量分析的关键,该算法通过对多能谱或多能段数据进行处理和分析,将复杂的混合材料分解为其组成的基本材料^[14]。1976 年,Alvarez 等^[15]首次提出双能 CT 技术,它利用同一物质在不同 X 射线能谱下衰减系数不同的特性成像,能够准确获得物质的等效原子序数和平均电子密度。基于投影域的算法是利用投影数据的物理特性和统计信息,通过优化算法或迭代重建技术,实现材料分解^[16]。查表法作为简单便捷的一种方法,Zhang 等^[17]利用标定好的投影衰减测量值建立查找表,对标定点进行线性插值得到了较好的投影分解结果,但在投影域分解中,分解结果受多能段数据的匹配一致性影响较大。随着硬件技术的进步和数据采集能力的提高,光子计数探测器(photon counting detectors, PCD)在 2013 年实现能量通道数突破,如 CERN 研发的 Medipix3 探测器支持 8 能量阈值^[18],使多材料分解成为可能。基于图像域的算法是在图像域利用多能 CT 图像间的线性或非线性的关系,通过解析数学模型或最小化重建误差的方式,实现材料分解和定量分析^[19-20]。针对图像域分解噪声激增的问题,Harms 等^[21]利用图像中相似像素的非局部信息进行噪声抑制,而非仅依赖边缘,通过计算像素邻域的相似性矩阵对噪声进行加权平均,并在优化目标中加入正则化项,较好地改善了在分解中对噪声的抑制能力,但其计算效率和偏差问题仍需优化。基于投影域和图像域的分解算法已经得到了广泛应用,但它们在处理伪影、噪声和计算效率方面存在一些限制。针对于此,研究人员开始探索直接迭代分解和基于深度学习的算法。在直接迭代分解算法中,研究人员通过迭代优化的方法,不断更新基材料的估计值,从而提高分解的准确性和稳定性^[22-23],这种方法可以有效应对伪影和噪声问题。Zhao 等^[24]利用

一阶 Taylor 级数展开,提出一种称为“EART”的扩展代数重建算法应用于双材料分解任务,算法较好地解决了非线性分解问题,但收敛速度较慢。另一方面,基于深度学习的能谱 CT 材料分解算法利用神经网络的强大建模能力和自适应特征学习能力,能够从大量的训练数据中学习到复杂的映射关系,实现高精度的能谱 CT 材料分解^[25-26]。Wu 等^[27]提出了一种基于改进的全卷积密集网络(FC-DenseNets)能谱 CT 多材料分解方法,旨在解决传统方法在高噪声下分解效果差的问题。虽然基于深度学习的方法在准确性和鲁棒性方面取得了显著的突破,但对于模型的解释性和泛化能力仍需要进一步研究和探索。

本文对近年来能谱 CT 在材料分解算法方面的研究进展进行了综述,重点介绍了基于投影域、图像域、直接迭代和深度学习的能谱 CT 材料分解算法。通过对这些算法的综合分析和比较,深入探讨了它们的优势、限制以及未来的发展方向,这将有助于进一步提高能谱 CT 的成像质量和材料分解的准确度,推动该领域的发展和应用。

1 能谱 CT 实现方式

能谱 CT 充分利用能谱信息,依据材料衰减系数对能量的依赖特性,在材料分解、物质识别方面有广阔的前景。目前能谱 CT 的实现方式主要有多次扫描、双源双探扫描、kVp 切换扫描、双层探测器扫描以及结合光子计数探测器扫描。图 1 为能谱 CT 常见的 5 种实现方式原理图。

多次扫描技术以 Canon Aquilion Precision 能谱 CT 为代表^[28]。多次扫描即以不同能量对被检测物进行扫描,获得多能投影数据。该方式实现简单,成本较低,但扫描时间延长,辐射剂量增大,空间分辨率较低。

双源双探扫描技术以 Siemens 公司的 SOMATOM Force 为代表^[29]。这种扫描方式要求两组 X 射线-探测器设备按一定角度交叉安装,两组设备在不同能量下同时对被检测物体进行扫描,一次扫描可以获得两组投影数据,缩短了扫描时间,但大大提高了成本。

kVp 切换扫描技术以 GE 公司的 Discovery 750HD 为代表^[30]。这种扫描方式要求射线源电压在极短时间内实现快速切换,配合具有高响应速度的探测器,可同时采集到不同能量的数据。此方式具有较好的成像视野,但难以同时调节电压电流,合理分配高低能数据采样数目同样也是难点所在。

双层探测器扫描技术以 Philips 公司的 IQon 为代

表^[31]。此类扫描方式的探测器采用两层不同材料构成,当X射线穿过第一层材料时,能量被部分吸收,能谱分布发生变化,等射线再进入第二层探测器即可获得两组不同能谱的X射线。该成像方式被认为是最接近光子计数型的能谱CT,但能谱区分能力有限。

上述扫描方式采用的是能量积分型探测器 (energy-integrating detector, EID),图2为能量积分(间接)和光子计数(直接)探测器原理对比图^[32]。EID的工作原理是利用闪烁体捕获入射光子,并激发出闪烁光子,光信号由光电倍增管收集并积分求出能量大小。而PCD以半导体材料为探测介质,一般为硅(Si)、砷化镓(GaAs)、碲化镉(CdTe)、碲锌镉(CdZnTe)等,利用半导体材料产生一个电子-空穴对所需要能量几乎固定这一物理性质,不同能量的入射光子产生不同数目的电子-空穴对,直接表现为不同幅值的电信号,再经放大器放大后与探测器设置的能量阈值相比较,可对入射光子进行计数,进而实现精确

的能谱测量。独特的物理性质使得光子计数型能谱CT在执行材料分解任务中具有先天优势,传统的能量积分型能谱CT实现形式一般可达到双能、三能已是极限,而PCD可将能区划分到3个以上,多能区的划分不仅可以有效隔绝电子噪声、降低辐射剂量、减弱硬化伪影,而且理论上能区间不存在重叠,进一步提高了材料定量分解的精度^[33-34]。此外,PCD可主动选取能量阈值,针对高Z物质可利用K-edge特性(K-edge称为K边,其物理意义是高原子序数物质原子内部K层自由电子,易与特定能量下X射线光子发生光电吸收作用,导致对该能量的X射线光子吸收特别大)成像,增强组织对比度,提高图像分辨能力^[35]。目前,国际上最具代表性的PCD包含美国Varex公司的DC系列^[36]、欧洲核子研究中心(Conseil Européenn pour la Recherche Nucléaire, CERN)研究的Medipix系列^[37]、瑞士Dectris公司的Pilatus^[38]系列产品以及日本滨松公司(Hamamatsu)的产品等^[39]。

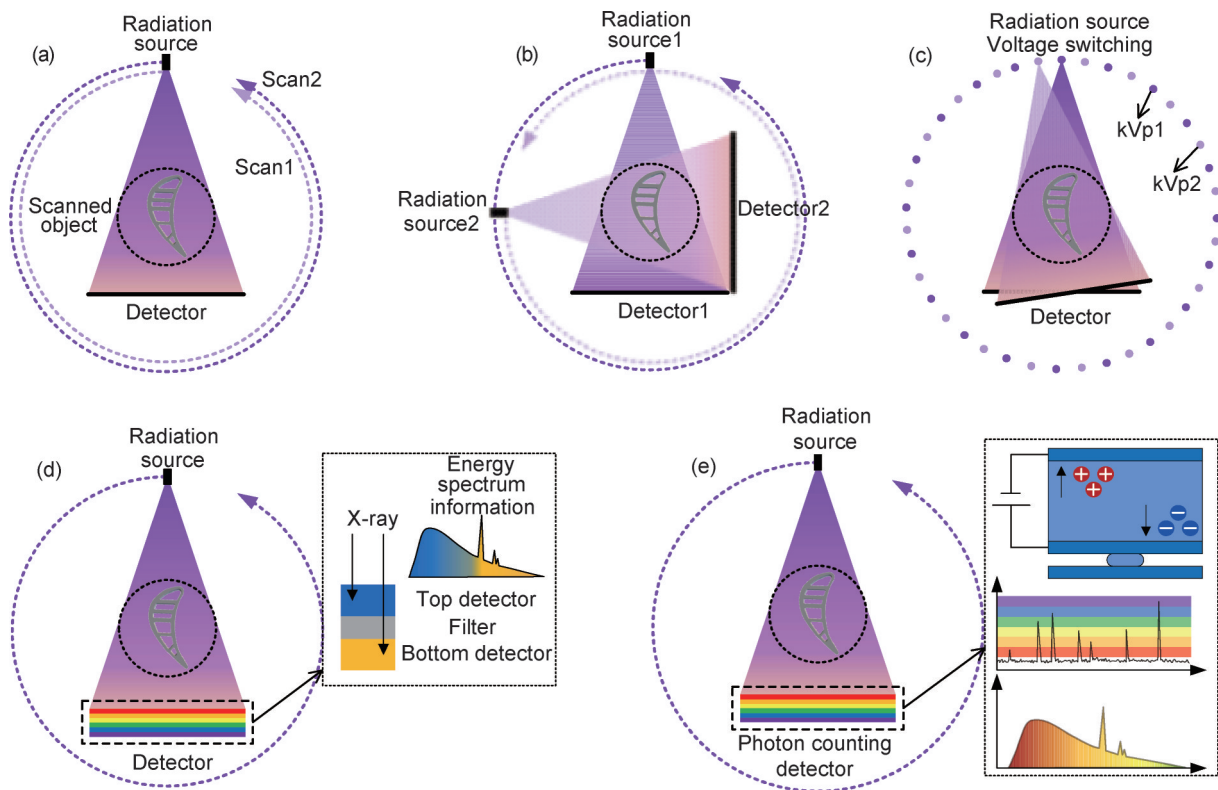


图1 能谱CT常见的5种实现方式原理图

(a)多次扫描;(b)双源双探扫描;(c)kVp切换扫描;(d)双层探测器扫描;(e)结合光子计数探测器扫描

Fig.1 Schematic diagrams of five common implementations of spectral CT

(a)multiple scans;(b)dual-source dual-probe scan;(c)kVp switching scan;(d)double-layer detector scan;(e)combined photon-counting detector scan

2 能谱CT材料分解数学模型

X射线穿透被测物体后,在考虑光子能谱和探测器响应函数的情况下,第 m 个能段的投影 p_m ,可用以

下数学模型表示:

$$p_m = -\ln \left(\int_{E_{\min}}^{E_{\max}} R(E_m) S(E_m) \exp \left[- \int_L \mu(l, E_m) dl \right] dE \right),$$

$$m = 1, 2, \dots, M \quad (1)$$

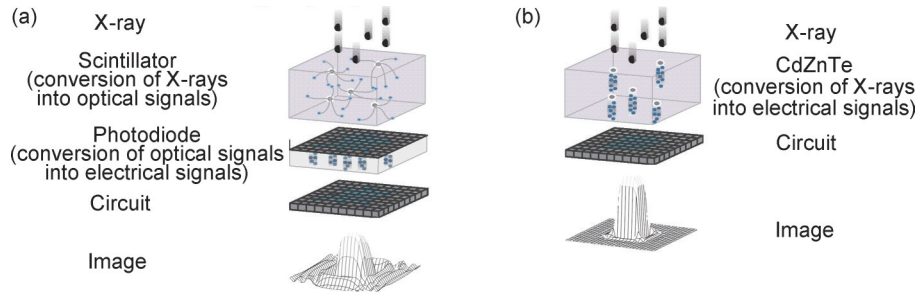


图 2 能量积分(间接)(a)和光子计数(直接)(b)探测器原理对比图^[32]

Fig.2 Schematic comparison of energy integrating (indirect)(a) and photon counting (direct) (b) detectors^[32]

式中： E_{max}^m 和 E_{min}^m 分别表示第 m 个能量通道下能量 E 的最大值与最小值； $R(E_m)$ 表示第 m 个能段的探测器响应函数； $S(E_m)$ 表示第 m 个能段的能谱信息； $\mu(l, E_m)$ 表示在第 m 个能段物质的线性衰减系数随能量 E 和位置 l 的分布。图 3 为锥束式能谱 CT 成像原理示意图，由图 3 能反映出式(1)的数学原理。

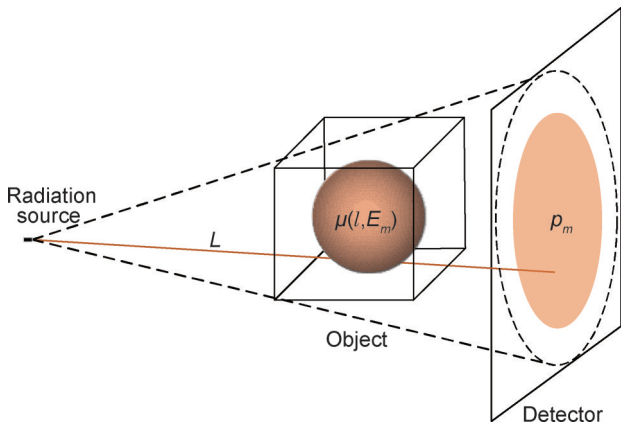


图 3 锥束式能谱 CT 成像原理示意图

Fig.3 Schematic diagram of cone-beam energy spectrum CT imaging principle

在执行能谱 CT 材料分解时，主要任务即为利用投影数据 p_m 求解出被测物体内部材料的衰减系数分布 $\mu(l, E_m)$ 。然而，由所采集得到的投影数据直接求解 $\mu(l, E_m)$ 这一过程是极度病态的，需要进行分解处理，通常可以将 $\mu(l, E_m)$ 近似表示为若干个基函数的线性组合：

$$\mu(l, E_m) \approx \sum_{k=1}^K \alpha_k(l) \tau_k(E_m) \quad (2)$$

式中： $\tau_k(E_m)$ 表示第 k 种预先标定基函数； $\alpha_k(l)$ 表示第 k 种基函数的对应权重。这样未知函数由求解 $\mu(l, E_m)$ 变为求解 $\alpha_k(l)$ 。

目前常用的线性组合分解模型有：双物理效应分解模型与基材料分解模型。双物理效应分解模型^[15]是将光电效应项 f_{ph} 和康普顿效应项 f_{kN} 作为基函数，即

$\tau_1(E_m) = f_{ph}(E_m)$, $\tau_2(E_m) = f_{kN}(E_m)$ ，通过求解相应的光电效应系数图像和康普顿效应系数图像，进而计算每个像素处的等效原子序数和平均电子密度，该模型适用性较强，但忽略了瑞利散射在光子衰减中的贡献，所以为近似模型。后者由 Kalender 等^[40]在 1986 年提出，该模型将 $\mu(l, E_m)$ 表示为若干种材料的质量衰减系数或线性衰减系数的组合，即 $\tau_k(E_m) = \mu_k(E_m)$ ，以此求解关注材料的体积分数分布或等效原子序数，这类模型相较于前者更加灵活，也更广泛地应用于医学图像重建等领域。具有 K-edge 效应的材料可以添加对应材料的基函数与这两种模型相结合^[41-42]。将式(2)带入式(1)得：

$$p_m = -\ln \left(\int_{E_{min}^m}^{E_{max}^m} R(E_m) S(E_m) \exp \left[-\sum_{k=1}^K A_k(L) \tau_k(E_m) \right] dE \right), \quad m = 1, 2, \dots, M \quad (3)$$

式中： $A_k(L)$ 表示为 $\alpha_k(l)$ 的积分值：

$$A_k(L) = \int_L \alpha_k(l) dl \quad (4)$$

能谱 CT 材料分解问题即转化为利用多能投影数据 $p_m, m = 1, 2, \dots, M$ ，求解出各基函数的分布 $\alpha_k(l), k = 1, 2, \dots, K$ ，这一方程组联合求解问题。在数学上，当 $M = K$ 时，是正定方程组求解，此时投影数等于基函数数目，常见于双能 CT 材料分解；当 $M < K$ 时，此时投影数小于基函数数目，是欠定方程组求解，这是实现多材料分解的主要问题，虽然可以通过质量分数守恒来增加约束，实现三材料分解^[43]，但该方法适用性不高，基于光子计数的能谱 CT 一次扫描可以获得多能投影数据，为解决此类问题带来了新的思路；当 $M > K$ 时，此时投影数大于基函数数目，是过定方程组求解。

3 能谱 CT 材料分解算法研究进展

基于投影域分解、基于图像域分解、直接迭代分解和基于深度学习分解是当前能谱 CT 材料分解算法

研究的主要方向,因此下面对这几类算法分别进行综合比较与分析。

3.1 投影域材料分解算法

投影域材料分解算法在采集得到的多能能谱数据基础上进行材料分解,通常将式(4)中的 $A_k(L)$ 视为质量密度 $\alpha_k(l)$ 沿射线路径 L 的投影,被定义为投影质量密度。假设采集的多能能谱数据能谱区间足够窄,可近似为单能射线,并忽略探测器单元响应不一致的情况,此时式(3)可近似表示为:

$$p_m \approx \sum_{k=1}^K \int_{E_{min}^m}^{E_{max}^m} S(E_m) \tau_k(E_m) dEA_k(L) = \sum_{k=1}^K \bar{\tau}_{k,m} A_k(L) \quad (m=1, 2, \dots, M \quad k=1, 2, \dots, K) \quad (5)$$

式中: $\bar{\tau}_{k,m}$ 表示第 k 种材料在第 m 能段时的加权平均衰减系数。此时投影域能谱CT材料分解算法可通过采集的多能投影数据 p_m 求解基材料的单色投影 $A_k(L)$,即:

$$\begin{pmatrix} p_1 \\ \vdots \\ p_M \end{pmatrix} = \begin{pmatrix} \bar{\tau}_{1,1} & \cdots & \bar{\tau}_{K,1} \\ \vdots & \ddots & \vdots \\ \bar{\tau}_{1,M} & \cdots & \bar{\tau}_{K,M} \end{pmatrix} \begin{pmatrix} A_1(L) \\ \vdots \\ A_K(L) \end{pmatrix}$$

$$\Downarrow$$

$$\begin{pmatrix} A_1(L) \\ \vdots \\ A_K(L) \end{pmatrix} = \begin{pmatrix} \bar{\tau}_{1,1} & \cdots & \bar{\tau}_{K,1} \\ \vdots & \ddots & \vdots \\ \bar{\tau}_{1,M} & \cdots & \bar{\tau}_{K,M} \end{pmatrix}^{-1} \begin{pmatrix} p_1 \\ \vdots \\ p_M \end{pmatrix} \quad (6)$$

得到多种基材料的投影数据 $A_k(L)$ 后,再利用常

规CT图像重建算法进行重建,得到基材料图像。图4为基于投影域的能谱CT材料分解算法流程示意图。

这类算法能够对多能投影进行准确建模,并且计算代价相对较低。然而,为了保证算法的有效性,多能投影数据的射线采集几何路径必须保持一致,否则会导致不同能区投影数据之间的匹配失败,从而无法实现材料分解,因此,该算法不适用于多源、多次扫描或高低能切换等能谱CT实现方式。同时,该类算法需要解决多能投影数据的非线性分解问题,以获取高质量的多种基材料投影数据成为该算法关注的重点。该类算法进一步可大致分为基于查表的方法和基于正则化与优化的方法。

针对投影分解中的非线性问题,基于查表的方法具有较高的效率,其中,李保磊等^[44]依据系统能谱与基材料线性衰减特性,建立了高低能投影与基材料投影间的数据查找表,查表找到最佳高低能投影匹配点,进而得到基材料分解投影,但其精度取决于查找表设定的步长。Zhang等^[45]提出一种基于局部加权线性回归查找表的迭代重建算法,此算法首先借助局部线性加权技术利用标定模型建立前向投影数据查找表,实现良好的局部信息标定,接着通过已建立的查找表,在迭代过程中寻找与投影数据最佳匹配的映射函数,进而迭代获得重建图像,实验结果验证了该方法具有良好的分解效果。

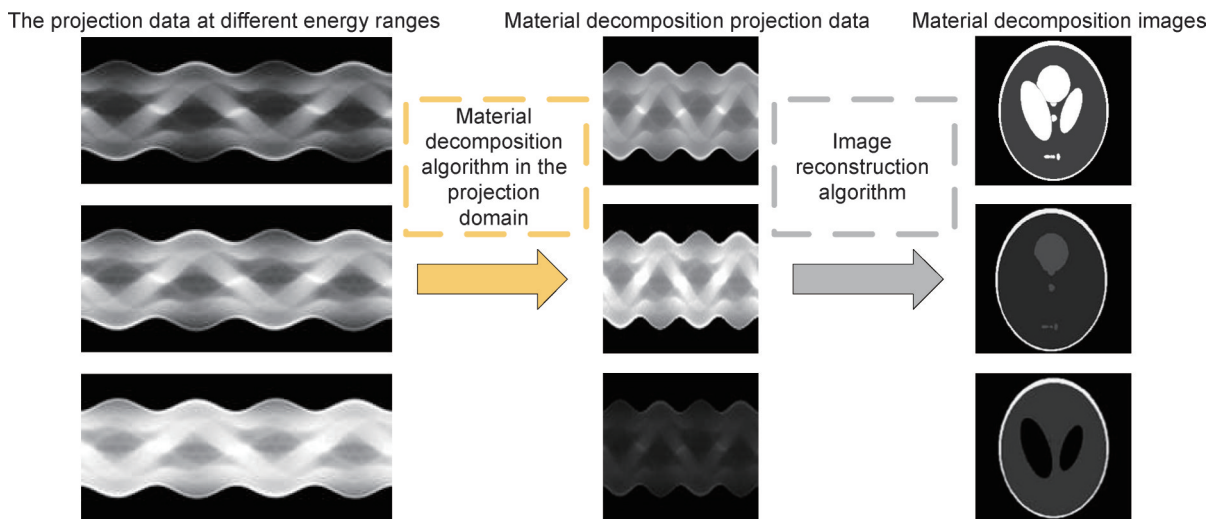


图4 基于投影域的能谱CT材料分解算法流程示意图

Fig.4 Schematic flow of energy spectral CT material decomposition algorithm based on projection domain

此外,还有一些研究者从正则化与优化的角度出发提高投影域材料分解能力。其中,Ducros等^[46]在投影域分解中引入了材料特性相关的正则化项,并采用

Gauss-Newton算法进行迭代求解,方法的有效性也在由五种材料组成的胸部模型中得到验证;Zhao等^[47]将测量数据视为统计上独立的泊松随机变量,基于最大

似然原理,建立了具有边缘保持正则化能谱分解权重向量和体积分数向量的约束优化问题,并在块坐标下降框架下,将问题分解为交替求解的二个子问题,利用优化转换原理优化问题,在能谱信息未知的情况下实现了投影分解。Cong等^[48]通过单变量优化双能CT投影分解,首先对相关指数函数进行奇次泰勒展开,得到一个奇次多项式方程,该方程在双能CT的上下文中具有唯一实数解,且精度足够用于图像重建,其次,通过单变量优化技术找到全局最优解,实现准确稳定的投影分解,但多项式方程和单变量优化的结合可能增加了模型的复杂性。Lu等^[49]提出了一种基于低秩和相似性正则化的投影域分解去噪算法,该方法基于惩罚加权最小二乘,利用双能段CT图像的结构冗余信息重构基材料图像,它借助张量的低秩特性以及结合基于相似性的正则化来实现,能够有效地保留精细结构和图像边缘,但此方法需要保证双能量投影的匹配性,否则会在图像边缘引入新的伪影,进而影响最终结果的准确性。图5为物理圆柱体模图^[49],其中1至5分别为聚丙烯PP、聚甲

基丙烯酸甲酯PMMA、聚甲醛POM、聚四氟乙烯PTFE和镁Mg,根据各材料电子密度和有效原子序数,选择PP和Mg分别作为低衰减和高衰减基材料^[21,49,50-52]。图6为低衰减和高衰减材料的不同材料分解算法结果对比图^[49],红框显示了低衰减基材料图像的局部放大图。

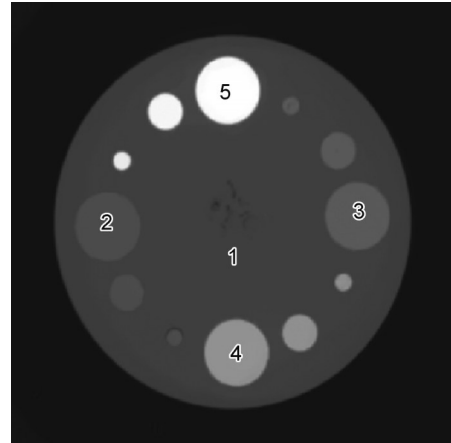


图5 物理圆柱体模图^[49]

Fig.5 Image of physical cylindrical phantom^[49]

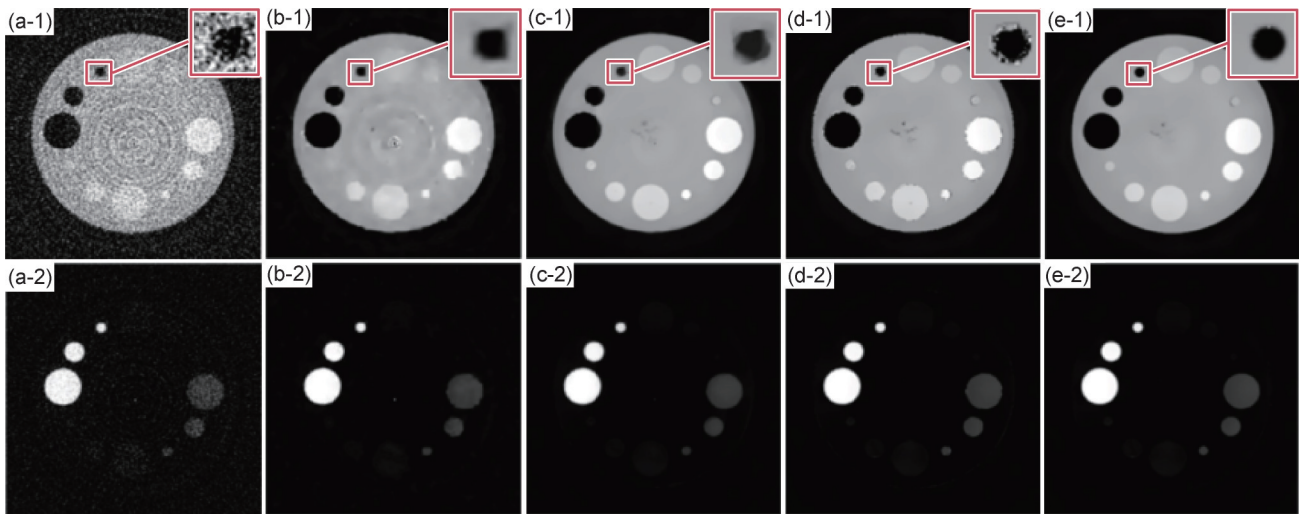


图6 低衰减(1)和高衰减(2)材料的不同材料分解算法结果对比图

(a)FBP^[50]; (b)DL^[51]; (c)PICCS^[52]; (d)SBR^[21]; (e)LRSBR^[49]

Fig.6 Comparison of results of different material decomposition algorithms for low attenuation(1) and high attenuation(2) materials

(a)FBP^[50]; (b)DL^[51]; (c)PICCS^[52]; (d)SBR^[21]; (e)LRSBR^[49]

综上所述,保证不同能段投影数据匹配性和实现复杂混合材料分解是投影域材料分解的难点和热点。PCD虽能够保证多能投影数据射线采集几何路径的一致性,但由于探测器响应不一致以及算法自身误差的影响,分解图像中会出现显著的环状伪影,从而严重影响此类算法的分解精度。因此,能谱CT中的环形伪影消除依然需要进一步研究。

表1^[17,44-49]为近年来基于投影域的能谱CT材料分解算法研究现状。

3.2 图像域材料分解算法

图像域材料分解算法先对多色投影数据 p_m 进行图像重建得到多能图像 I_m ,再利用图像域材料分解算法对多能图像 I_m 进行材料分解,得到基材料分解图像 a_k ,此时式(6):

表1 基于投影域的能谱CT材料分解算法研究现状

Table 1 Current status of research on projective domain-based energy spectral CT material decomposition algorithms

Time	Method	Suitable task	Advantage	Limitation	Ref.
2008	Based on a lookup table	Dual-material decomposition	It exhibits excellent reconstruction precision and accuracy, coupled with strong practical utility	Limited noise and artifact suppression capabilities	[17]
2011		Dual-material decomposition	It is easy to implement and facilitates parallel computing	The accuracy depends on the set step size of the look-up table, and the robustness of the algorithm requires further verification	[44]
2023		Dual-material decomposition	It does not rely on the system's energy spectrum or attenuation properties, and takes into consideration factors like scattering	The calibration model and the test object need to have the same material density	[45]
2017	RWLS-GN	Multi-material decomposition	It converges rapidly and is easy to parallelize for computation	Dependent on the selection of regularization parameters	[46]
2022	Based on blind separation	Dual-material decomposition	Does not rely on system energy spectrum info, facilitating parallel computation	Dependent on the selection of regularization parameters	[47]
2022	Based on univariate optimization	Dual-material decomposition	It demonstrates high accuracy and robust stability	The model is relatively complex	[48]
2024	PWLS-LRSBP	Dual-material decomposition	Effectively reduces noise levels while preserving image structural edges	It is necessary to ensure precise matching of dual-energy projections, as the parameters within the algorithm have a significant impact on the results	[49]

$$\begin{aligned}
 \begin{pmatrix} I_1 \\ \vdots \\ I_M \end{pmatrix} &= \begin{pmatrix} \bar{\tau}_{1,1} & \cdots & \bar{\tau}_{K,1} \\ \vdots & \ddots & \vdots \\ \bar{\tau}_{1,M} & \cdots & \bar{\tau}_{K,M} \end{pmatrix} \begin{pmatrix} a_1(L) \\ \vdots \\ a_K(L) \end{pmatrix} \\
 &\Downarrow \\
 \begin{pmatrix} a_1(L) \\ \vdots \\ a_K(L) \end{pmatrix} &= \begin{pmatrix} \bar{\tau}_{1,1} & \cdots & \bar{\tau}_{K,1} \\ \vdots & \ddots & \vdots \\ \bar{\tau}_{1,M} & \cdots & \bar{\tau}_{K,M} \end{pmatrix}^{-1} \begin{pmatrix} I_1 \\ \vdots \\ I_M \end{pmatrix} \quad (7)
 \end{aligned}$$

图7为基于图像域的能谱CT材料分解算法流程示意图。图像域材料分解算法优势是仅对重建后的CT图像处理,避免了投影域操作可能会引入的额外误差,实现较为简单,对多色投影数据射线采集的几何路径一致性要求不高,不受扫描方式限制,是现有能谱CT成像技术中应用最为广泛的一类算法。然而目前此类算法对于噪声和伪影的鲁棒性较差,在分解过程中存在噪声叠加问题,且基材料分解依靠像素之间的直接映射,该映射方式难以消除因投影域数据缺陷而产生于重建图像中的自身结构性伪影^[53],上述因素严重影响了最终分解图像的质量,是此类算法亟需解决的关键所在。这类算法进一步可大致分为基于图像的噪声分布特性、基于等效原子序数测量、图像域迭代分解和基于字典学习的分解方法。

在利用图像噪声分布特性进行材料分解的研究领域,Hao等^[54]提出1种基于参考图像的能谱CT图像

优化算法,该算法以低能图像作为参考,运用非局部像素相似性度量方法从参考图像中提取结构信息,进而确定目标图像相应位置的权重关系,此方法取得了较好的重建效果;Jiang等^[55]分析了多材料分解过程的噪声分布特性,提出了1种不改变基材料图像纹理的噪声抑制方法,该方法针对多能图像噪声分布特性制定相应抑噪方案,显著提升了基材料图像质量,然而在实际成像中,噪声分布特征的精确描述极具挑战性,因此对噪声抑制十分受限。

CT图像表征每个像素内材料的线性衰减系数分布情况,而相较于材料衰减系数,等效原子序数可以更好地体现材料内部组成。对此,杨亚飞等^[9]提出了1种等效原子序数测量方法,推导了2个能量区间线性衰减系数之比与等效原子序数的关系,在保证算法鲁棒性与稳定性的同时,大幅降低设备要求和算法复杂度,对含能材料的成分检测和生产工艺改进具有重要意义。李思宇等^[56]通过构建三阶拟合模型来快速准确地估计基材料的等效原子序数与密度,并将这一方法应用于青铜器检测,在一定程度上反映了青铜器内部锈蚀情况。Jumanazarov等^[57]提出了一种基于能谱CT的材料分解方法,利用多项式曲线拟合等技术估算目标材料的有效原子序数,实现聚乙烯、聚氯乙烯和水等材料的检测。

同时有结果表明,在图像域进行迭代分解不断更

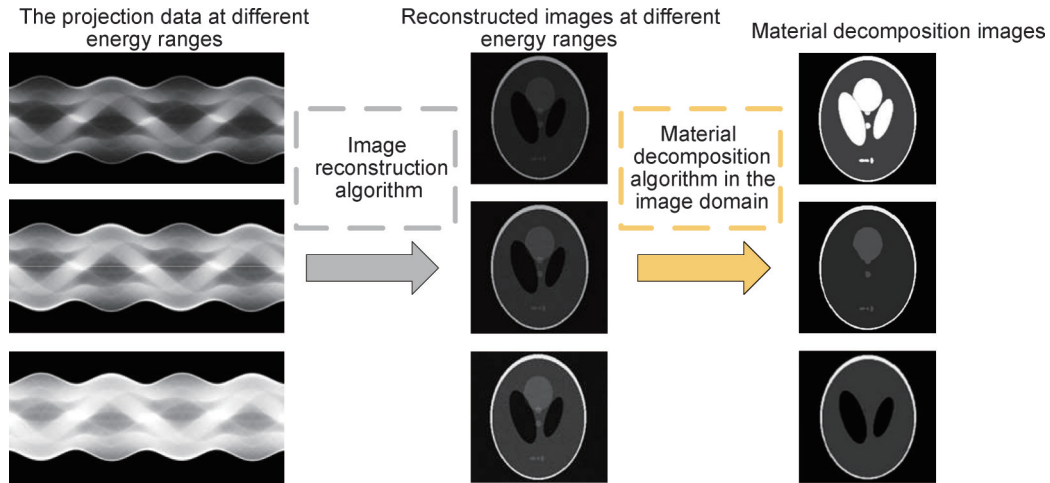


图 7 基于图像域的能谱 CT 材料分解算法流程示意图

Fig.7 Schematic flow of energy spectral CT material decomposition algorithm based on image domain

新基材料图像直至收敛,可以更大程度抑制噪声。Niu 等^[58]提出了一种经典的图像域迭代分解算法,该算法将噪声方差-协方差矩阵的倒数作为最小二乘目标函数的惩罚加权,并结合边缘加权正则化,利用共轭梯度法对模型迭代优化,获取较好噪声抑制性能的同时还较准确地保持了图像边缘信息。该算法较好地实现了双材料分解任务,但并未完整刻画多能图像与基材料图像之间的映射关系,一些情况下难以清晰地区分不同组织对象的边界分布。大于两种基材料的分解任务在实际需求中十分普遍,针对此问题, Mendonca 等^[59]提出基于质量和体积分数守恒的能谱 CT 逐像素多材料分解算法,其算法假定单个像素内基材料体积分数之和恒定,借助这一约束条件,实现了多材料分解任务。Xue 等^[53]在上述研究方法的基础上继续拓展,在原模型基础上结合了先验统计信息,并引入 1 种统计映射关系,用于描述不同能量下物质的吸收特性,通过建立这一映射关系,能够更准确地估计不同材料的成分、密度信息。Zhou 等^[60]提出一种基于最大后验期望最大化的图像域迭代分解算法,该算法通过最大化后验概率来更新基材料图像的估计值,通过反复迭代,最终获得高质量的重建图像。

随着压缩感知理论的发展,基于字典学习的方法正被广泛研究。Wu 等^[61]将字典学习方法引入图像域材料分解任务中,利用训练好的字典来搜索分解后材料图像的相似度,为分解模型增加更多约束,此方法在三种基材料分解和定量分析任务中具有较好性能。Xie 等^[62]结合了多种约束进行图像域材料分解,取得的分解效果比常见的 l_1 范数约束稀疏正则化方法更准确。Zhang 等^[63]提出一种结合稀疏残差先验和字典学习的图像域材料分解算法,该算法保留了字典学习的

抗噪优势,针对字典学习在保持精细结构和边缘信息方面的不足,引入基于像素值的 l_0 范数约束,借助先验图像和材料图像间的结构冗余信息引导材料分解过程,进一步提高了边缘保持能力与材料分解精度。图 8 为骨、软组织和碘的不同材料分解算法结果对比图^[51,61-62]。

综上所述,图像域材料分解算法受噪声和伪影的影响较大,因此,在此类算法基础上引入图像先验信息,对材料分解问题加以约束,提升算法鲁棒性和可靠性将是该领域的发展趋势。此外,将能谱 CT 与其他成像模态(如 CT、核磁共振成像等)相结合,借助多模态数据的互补信息获得更全面和准确的材料分解结果,也将成为研究热点。表 2^[9,53-58,61-63]概述了近年来基于图像域的能谱 CT 材料分解算法研究现状。

3.3 直接迭代分解算法

直接迭代分解算法利用多色投影数据直接实现材料分解,又被称为一步反演法。不同于投影域和图像域的材料分解算法,一步法结合了重建和分解过程,相比于两步法减少了中间多次级联可能导致的信息损失。但如何对非线性数据模型进行优化求解,抑制分解过程中的噪声,提升算法的收敛性和稳定性,是该类算法的主要问题。该类算法进一步可大致分为基于代数重建方法和基于正则化与稀疏优化方法。图 9 为基于直接迭代的能谱 CT 材料分解算法流程示意图。

在原代数重建算法基础上,受 EART 方法^[24]启发,近年来基于 EART 衍生出多种变体,如 Hu 等^[64]提出 1 种称为“ESART”的扩展同步代数重建算法,该算法加快了收敛速度,同时具有更好的抑噪性能;Zhang 等^[65]提出了一种基于单色图像引导的迭代重建算法,

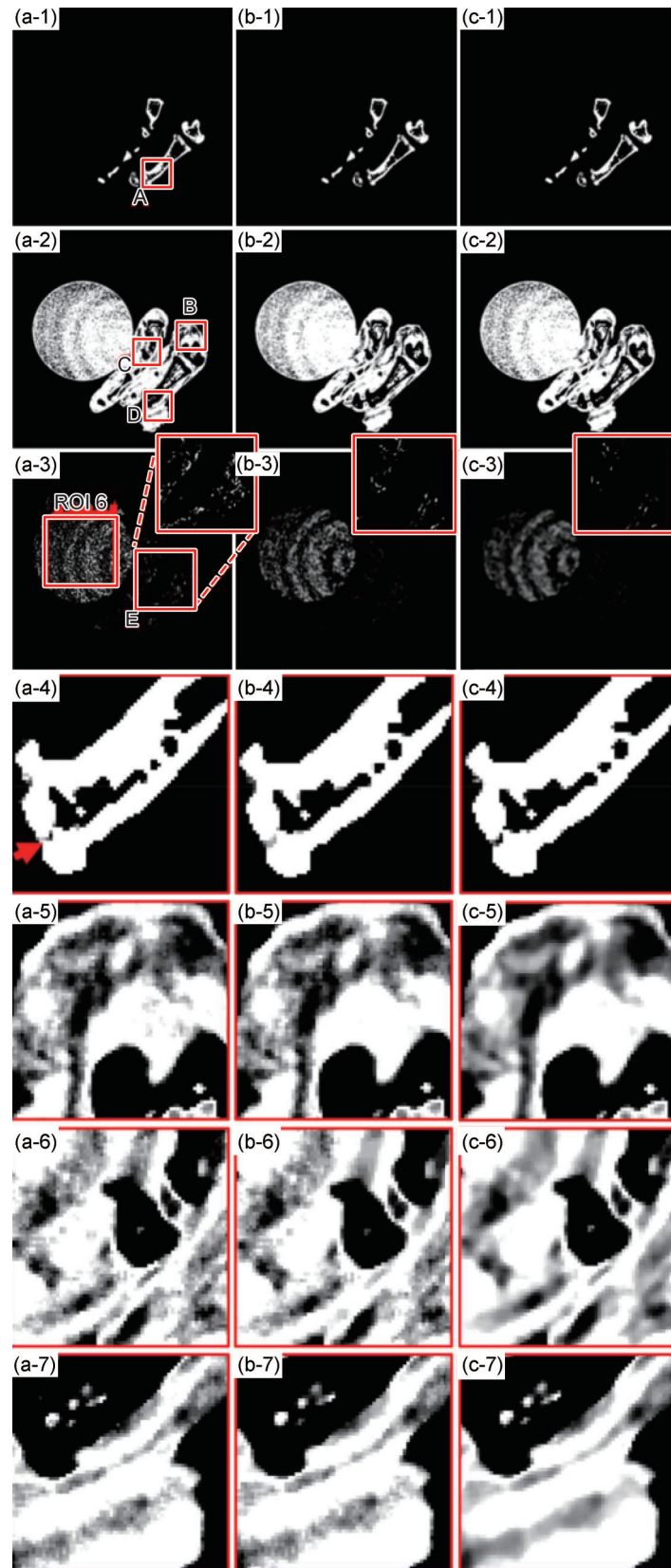


图8 骨(1)、软组织(2)和碘(3)的不同材料分解算法结果对比图,及A~D区域放大图(4)~(7)算法
(a)DL^[51]; (b)TVMD^[62]; (c)DLIMD^[61]

Fig.8 Comparison of results of different material decomposition algorithms for bone(1), soft tissue(2), and iodine(3), and enlarged views of regions A-D(4)-(7)
(a)DL^[51]; (b)TVMD^[62]; (c)DLIMD^[61]

表 2 基于图像域的能谱 CT 材料分解算法研究现状

Table 2 Current status of research on image-domain based energy spectral CT material decomposition algorithms

Time	Method	Suitable task	Advantage	Limitation	Ref.
2013	Based on the noise distribution	Dual-material decomposition	It has achieved good results in noise suppression and artifact removal	The algorithm has high complexity	[54]
2019	characteristics of the image	Multi-material decomposition	Significantly reduces noise and achieves high-precision material decomposition	There are certain limitations in its ability to retain details	[55]
2022	Measurement of equivalent atomic number	Multi-material decomposition	Low equipment requirements and algorithm complexity, coupled with strong robustness	The generalization performance requires further verification, and calibration tests and measurement experiments need to be conducted under the same conditions	[9]
2024		Multi-material decomposition	Capable of rapid and accurate estimation of equivalent atomic number and density	The applicability to other complex materials needs further verification	[56]
2023		Multi-material decomposition	Exhibits good robustness and generalization capabilities	It is affected by the number of energy intervals and base materials	[57]
2014	Iterative decomposition in the image domain	Dual-material decomposition	It offers excellent noise suppression while preserving image edge details accurately	The mapping relationship between multi-energy images and base material images is not fully characterized	[58]
2017		Multi-material decomposition	It demonstrates a high level of decomposition precision and accuracy	The algorithm requires an appropriate initial value, and the selection of this initial value has a significant impact on the results	[53]
2021		Dual-material decomposition	Exhibiting good noise suppression performance and high decomposition precision	Without comparative experiments, the practicality needs further verification	[60]
2020	Dictionary-based learning	Multi-material decomposition	High quantitative decomposition precision and accuracy	The applicable scope may be limited by the diversity and quantity of dictionary samples	[61]
2019		Multi-material decomposition	The introduction of multiple constraints has significantly improved decomposition precision and accuracy	It depends on the selection of regularization parameters and initial values	[62]
2023		Multi-material decomposition	While accurately decomposing base materials, it also exhibits good performance in noise reduction and edge preservation	It relies on the selection of regularization parameters and has high computational complexity	[63]

此方法进一步提升了收敛速率。Zhao 等^[66]提出一种斜投影修正技术,能够在不一致扫描情况下实现材料分解;在上述研究的基础上,Pan 等^[67]提出一种 Schmidt 正交修正算法,对投影数据进行正交修正,从而加速了迭代过程;Yu 等^[68]针对不一致扫描情况下的多材料分解问题,通过引入体积守恒约束,并将能谱 CT 成像不一致性问题建模为正则化项,嵌入到多材料重建分解过程中,进一步提高了分解结果的准确性。

利用先验知识构建数据正则化项是此类算法抑制噪声的常用手段,此外,现有研究显示,采用基于稀疏性的迭代算法可进一步提升重建质量。如 Cai 等^[69]

在贝叶斯重建算法中采用 Huber 函数(Huber 函数是一种在统计学、图像处理等领域广泛应用的函数,用于平衡数据拟合中的平滑性和对异常值的鲁棒性)作为正则化项;Long 等^[70]在统计迭代重建方法中,基于惩罚似然函数和边缘细节保持来构建正则化;Barber 等^[71]将含有凸优化的原始对偶算法应用于能谱 CT 材料分解任务中,并将似然函数与全变分(total variation, TV,在图像处理领域,全变分用于描述图像中像素值的变化程度。图像平滑区域的全变分小,而边缘、纹理等变化丰富的区域全变分大)正则化模型相结合,一定程度上解决了数据模型的非凸问题。在此

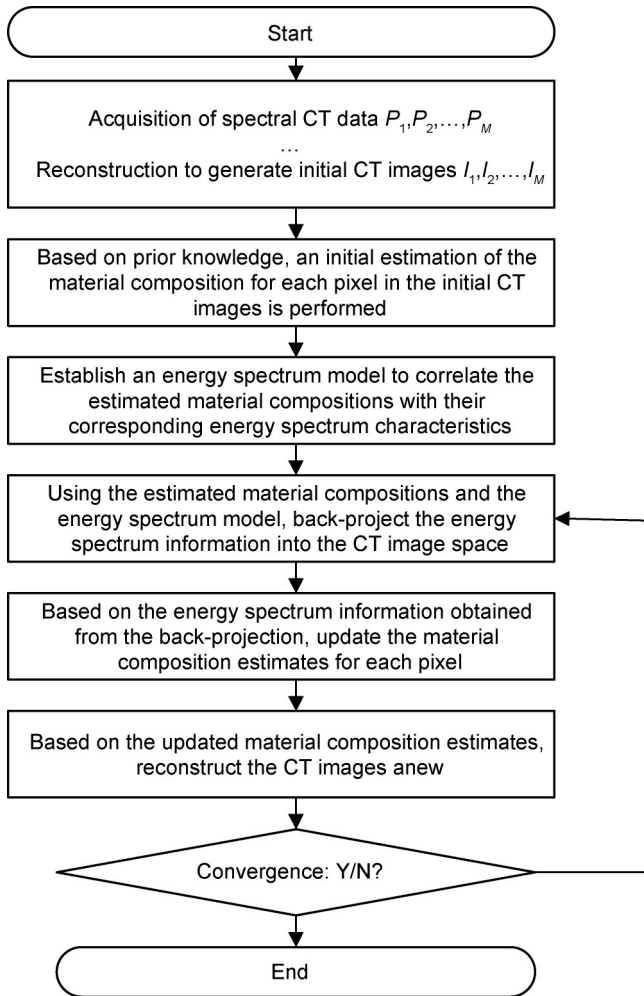


图9 基于直接迭代的能谱CT材料分解算法流程示意图

Fig.9 Schematic flow of direct iterative energy spectral CT material decomposition algorithm

基础上,他们进一步提出非凸交替方向乘子法^[72],该方法可用于解决更复杂的非凸问题,并应用于光子计数CT系统重建,有效地减少了射束硬化和金属伪影^[73];Zhang等^[74]将TV正则化与BM3D框架相结合,对双材料分解过程中的噪声伪影进行了较好地抑制。然而,基于原始对偶框架算法收敛效果并不令人满意,在处理多材料分解任务时,存在病态性加剧、过程不稳定以及需要手动调整正则化项参数等问题。针对这些情况,Yu等^[75]引入自适应步长控制和正则化选择机制,提出1种自适应的多材料直接重建算法,在保证重构精度的同时提高了计算效率。Yang等^[76]结合异性引导滤波器和 l_0 范数,借助异性稀疏变换进行能谱CT图像重建,在降噪和边缘保留方面取得了更好的平衡,但其算法复杂度较高,计算效率低。表3^[24,64-71,74-76]概述了近年来基于直接迭代的能谱CT材料分解算法研究现状。图10为水、肌肉和骨头的不同材料分解算法结果对比图^[24,66,68,74,71]。

综上所述,直接迭代分解算法可以更准确地建模能谱数据和材料成分之间的关系,但其面临收敛速度慢、噪声抑制不足、算法稳定性差以及计算效率低等问题。因此,如何提升该算法收敛性和稳定性,以提高材料分解的准确性和鲁棒性仍然是该领域一个重要的研究方向。

3.4 基于深度学习的材料分解算法

近年来,深度学习被广泛应用于图像分割^[78]、分类^[79]、目标检测^[80]、图像去噪^[81]和伪影消除^[82]等领域。大量研究表明,深度学习凭借其强大的特征学习与分层特征提取能力,能够有效解决图像分割问题。同样,利用深度学习强大的映射能力,可构建多能图像 I_M 与基材料图像 a_K 之间的映射函数。这类算法可以进一步细分为两大类:一类是基于常规能谱CT直接实现材料分解的方法,另一类是基于单能CT生成多能图像,进而实现材料分解的方法。

目前,已有研究表明深度学习可以应用于能谱CT材料分解任务中。Chen等^[83]基于VGG16网络在Sheep-Logan模型上与传统方法进行多材料分解效果对比,取得了更优异的结果,验证了深度学习方法执行材料分解任务的可行性与优越性;Clark等^[84]提出基于U-net网络的能谱CT材料分解方法,在仿真实验中稳健地实现了多材料分解;Xu等^[85]提出1种由卷积层和全连接层组成的级联式神经网络来解决材料分解问题,实验结果表明深度学习方法在解决非线性问题方面极具前景;Zhang等^[86]提出1种蝶形网络,该网络衍生于图像域基材料分解模型,网络中的交叉架构有效实现了两种材料间的信息交互,增强了学习方法执行材料分解过程的可解释性;Su等^[87]提出1种名为DIRECT-Net的端到端神经网络模型,该网络可联合使用投影域正弦图和切片域CT图像的先验信息来实现精确的双材料分解。卷积神经网络(convolutional neural networks, CNN,是1种专门为处理具有网格结构数据而设计的深度学习模型,由卷积层、池化层和全连接层等基本结构组成)显著提升了材料分解精度,但传统CNN卷积算子可能限制从CT图像中提取非局部特征。对此,Shi等^[88]将多尺度非局部自相似模式的图模型引入到材料分解过程中,提出1种基于图像边缘条件卷积U-net的多材料分解网络,该网络既能借助图像神经网络提取CT图像的非局部空间特征,又能保留CNN提取的图像局部信息。受Goodfellow等^[89]提出的生成对抗网络(generative adversarial network, GAN,由生成器和判别器构成,二者相互对抗、学习,在不断的博弈过程中提升性能)启发,Geng等^[90]提出1种并行多流生成对抗网络方法,该方法利

表 3 基于直接迭代的能谱 CT 材料分解算法研究现状

Table 3 Current status of research on direct iterative-based energy spectral CT material decomposition algorithms

Time	Method	Suitable task	Advantage	Limitation	Ref.
2014	EART	Dual-material decomposition	It demonstrates good performance in terms of image quality and artifact suppression	Low computational efficiency	[24]
2016	ESART	Dual-material decomposition	It exhibits superior reconstruction quality and accuracy, while enhancing convergence rates	The success of this method relies partly on data quality and preprocessing strategies	[64]
2021	IRM-MI	Dual-material decomposition	It can be utilized for monochrome image decomposition, significantly improving convergence rates	Limited artifact suppression capability	[65]
2021	OPMT	Dual-material decomposition	It is applicable to inconsistent scanning situations	The robustness in dealing with noise and artifacts has not been thoroughly discussed	[66]
2023	SOMA	Multi-material decomposition	It can accurately decompose base material images, significantly enhancing convergence rates	The influence of scattering was neglected during method modeling	[67]
2024	Based on volume conservation constraint	Multi-material decomposition	It is suitable for inconsistent scanning situations, effectively suppressing noise	The algorithm model is based on assumptions, and its robustness requires further validation	[68]
2013	Based on full-energy spectrum bayesian	Dual-material decomposition	It possesses high decomposition accuracy and demonstrates robustness against noise and material variations	There is an issue of detail loss, and the edge preservation capability is poor	[69]
2014	Based on penalized likelihood	Multi-material decomposition	It effectively suppresses noise, stripes, and cross-contamination artifacts	High computational complexity	[70]
2016	Primal-dual problem with convex set constraints	Dual-material decomposition	To some extent, it addresses the non-convexity of the data model	The ability to preserve fine structures is limited, and the robustness of the algorithm requires further validation	[71]
2019	TV+BM3D	Dual-material decomposition	It has good capability in preserving image details and texture information	There remains the issue of image edge distortion	[74]
2023	Iterative proximal adaptive descent	Multi-material decomposition	While achieving multi-material decomposition, it effectively suppresses noise and beam-hardening artifacts	The algorithm model is based on assumptions, and its robustness needs further validation	[75]
2024	AST	Multi-material decomposition	It offers high decomposition accuracy and is capable of preserving structural edges while reducing noise	The algorithm has high complexity and requires a long processing time	[76]

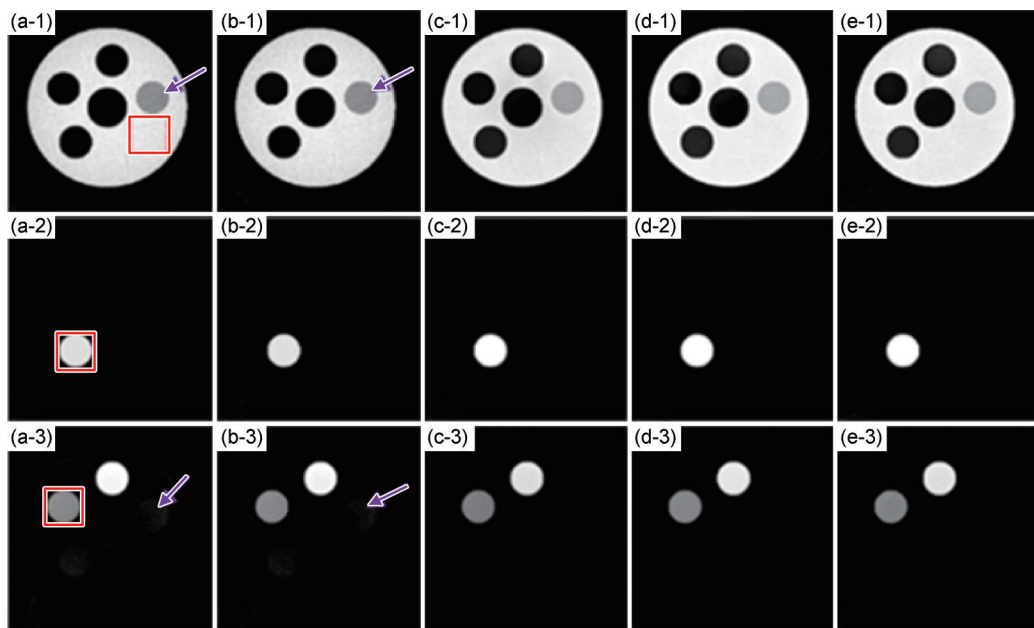


图 10 水(1)、肌肉(2)和骨头(3)的不同材料分解算法结果对比图 (a)EART^[24]; (b)OPMT^[66]; (c)DnCNN^[77]; (d)TV^[74]; (e)VCC^[68]

Fig.10 Comparison of results of different material decomposition algorithms for water(1), muscle(2) and bone(3)

(a)EART^[24]; (b)OPMT^[66]; (c)DnCNN^[77]; (d)TV^[74]; (e)VCC^[68]

用多个生成器来生成各自对应的基材料图像,是1种高效准确的多材料分解方法。与传统卷积神经网络相比,GAN可更有效地保留纹理细节特征,但庞大的模型通常会出现模态坍塌、网络收敛效率等问题,对此,Shi等^[91]提出一种双交互式 Wasserstein GAN 双材料分解算法,该算法通过交替训练两个生成器,来提高分解结果的准确性和稳定性,并有效抑制噪声和伪影。多能段阈值可划分是光子计数能谱CT系统的独有优势,然而在狭窄的能段中存在大量量子噪声,使得CT图像的灰度值表征不准确,进而影响材料分解的准确性,为解除这一限制,Guo等^[92]提出1种基于注意力机制的全局卷积生成对抗网络,该方法结合空间和通道注意力机制,可准确分割能谱CT图像中的不同组织成分,取得了优异的分解效果。

双能CT、光子计数型能谱CT在提供材料特征信息方面具有巨大潜力,然而单能CT仍是全球使用最广泛的CT系统。对此,Lyu等^[93]基于深度学习方法,在训练阶段,利用去噪的双能CT图像和单视图双能投影来训练投影域CNN和MD-CNN,在测试阶段,训练好的网络凭借输入的低能图像和单视图双能投影推断相应的高能图像。Koike等^[94]提出基于AI的图像域材料分解方法,借助虚拟单色图像的多keV输出学习,从单能CT图像中创建双能CT等效图像,实验结果表明,即便没有双能CT系统,单能CT系统依靠深度学习方法执行材料分解也是可行的。这一研究有助于进一步降低当前双能CT设备的辐射剂量,且利用单能CT设备实现双能CT成像,可简化材料分解的实现成本。然而,由原始的单能图像合成另一张单能图像,进而形成双能CT图像并最终生成材料分解图,这不是个简单的过程,其中诸多步骤可能会引入误差。针对此,Wang等^[95]提出一种改进的GAN模型,其中生成器结合了CNN和Transformer,该方法可从传统的单能CT图像中直接生成材料分解图像,对照实验也验证了该方法的优异性与鲁棒性。表4^[83,88,90-95]概述了近年来基于深度学习的能谱CT材料分解算法研究现状。图11为水、钙和碘的不同材料分解算法结果对比图^[27,84,88,96]。

综上所述,深度学习在材料分解领域已取得了瞩目的成就。然而,深度学习模型的训练往往高度依赖于大规模的标注数据集,在实际应用场景中,获取充足且准确的标注数据往往是一项艰巨的任务。鉴于此,探索解决数据稀缺性和标注难题的途径,开发高效的深度学习算法,成为该领域一个亟待攻克的重要

研究方向。迁移学习作为1种前景广阔的技术手段,在面临大规模标签数据集缺失的情况下,能够展现出其独特优势。通过迁移学习,可以将已在一个任务上成功训练的模型知识迁移到另一个相关任务上,从而利用既有知识提升算法的性能^[97-98]。然而,迁移学习的应用也面临挑战,诸如不同任务和数据集间可能存在领域差异,以及如何制定恰当的知识迁移策略等。因此,在能谱CT材料分解算法中,迁移学习机遇与挑战并存,未来需深入研究探索,不断优化算法性能,增强泛化能力,进一步推动深度学习在材料分解领域的应用与发展。

4 结束语

能谱CT是1种通过测量物体的能谱信息来获取其材料成分的成像技术。材料分解算法是能谱CT中的关键步骤,它将能谱数据转化为材料组成成分图像。本文对近年来不同类别能谱CT材料分解算法的研究进展进行了概述分析,总体上能谱CT的材料分解需求明确并发展迅速,目前已经取得了许多创新性成果,但仍存在一些问题需要进一步研究和解决。

(1)保证多能段投影数据匹配性和实现复杂混合材料分解是投影域分解的发展方向。该算法能对多能投影进行准确建模,但在处理复杂混合材料(如重叠或接触材料)时受限,且受多色投影数据射线采集的几何路径一致性影响。PCD的发展提高了这类算法的适用性,但探测器响应不一致和算法误差导致环状伪影,影响分解精度。因此,需进一步提高复杂混合材料分解能力和消除环形伪影的方法。

(2)引入图像先验约束和多模态数据相结合是图像域分解的主要趋势。此类算法直观显示基材料分布,但对于噪声和伪影敏感。引入图像先验信息可提升算法的鲁棒性和可靠性,是潜在的发展方向。此外,将能谱CT与其他成像模态(如CT、核磁共振成像等)相结合,利用多模态数据的互补信息以获得更全面和准确的材料分解结果同样至关重要。

(3)提高算法的收敛性和稳定性是直接迭代分解的重要研究方向。直接迭代分解算法相比于两步法减少了中间多次级联可能导致的信息损失,但其面临收敛速度慢、计算复杂度及算法稳定性差等问题。因此,深入研究提升算法收敛性和稳定性的方法,以提高材料分解的准确性和鲁棒性,仍然是该领域的重

表 4 基于深度学习的能谱 CT 材料分解算法研究现状

Table 4 Current status of research on deep learning-based energy spectrum CT material decomposition algorithms

Time	Model	Suitable tasks	Advantage	Limitation	Ref.
2019	VGG16	Multi-material decomposition	It exhibits high decomposition accuracy and robustness, with low training costs	The applicability and scalability of the method require further validation	[83]
2018	U-net	Multi-material decomposition	It is straightforward to implement and holds promise for application in various clinical and research fields	The method lacks noise suppression capability	[84]
2018	FCN+FCL	Dual-material decomposition	It demonstrates high decomposition accuracy and efficiency	The improvement in edge preservation capability is not significant, and the training cost is relatively high	[85]
2019	Butterfly network	Dual-material decomposition	Greater interpretability and better noise suppression performance	The generalization performance is limited, and when experimental parameters change, retraining is required	[86]
2022	DIRECT-Net	Dual-material decomposition	The decomposition results exhibit high image quality and decomposition accuracy	The implementation of dual-energy CT with inconsistent scanning paths is difficult to apply, and the training cost is relatively high	[87]
2024	GECCU-net	Multi-material decomposition	Good fine structure preservation capability and noise suppression ability	The generalization ability needs further validation, and the training cost is relatively high	[88]
2020	PMS-GAN	Multi-material decomposition	Generating multi-material images in parallel can reduce computation time and improve efficiency	When multiple generators operate in parallel simultaneously, the computational complexity is relatively high	[90]
2021	DIWGAN	Dual-material decomposition	While effectively achieving material decomposition, it suppresses noise and beam-hardening artifacts, demonstrating good robustness and stability	There are too many manually adjustable parameters, leading to high training costs	[91]
2023	AGC-GAN	Multi-material decomposition	While maintaining high resolution, it avoids artifacts and blurring effects that occur in traditional methods	The applicability and robustness of the method require further validation	[92]
2021	FLESH-DECT	Multi-material decomposition	It does not require dual-energy CT scanning, reducing scanning costs, and has the potential to simplify system design and lower radiation doses	Depends on high-quality training data	[93]
2024	AI (2D U-net)	Dual-material decomposition	Without the need for a dual-energy CT system, it offers high flexibility and ease of implementation	The generalization of the method needs further validation, and the selection and optimization of parameters are relatively difficult	[94]
2022	Improved-GAN	Multi-material decomposition	It realizes the mapping relationship from monoenergetic CT images to material decomposition images, reducing errors in the two-step synthesis process	It is necessary to use lightweight models and simplified parameters for large-scale pre-training	[95]

要研究方向。

(4) 迁移学习和高泛化性将是基于深度学习的材料分解算法的发展趋势。深度学习通过强大的特征提取能力, 构建多能图像与基材料图像之间的映射模型, 但其效能往往依赖大量标注数据。在实际工作中, 数据难以获取, 迁移学习可弥补数据不足的问题,

进而提高算法性能。然而, 不同任务和数据集之间存在领域差异, 以及知识迁移策略的合理选择, 构成了迁移学习在该领域应用的主要挑战。因此, 迁移学习在能谱 CT 材料分解算法中具有巨大的机遇和挑战, 需进一步研究以提升算法性能和泛化能力, 推动其在材料分解领域的应用与发展。

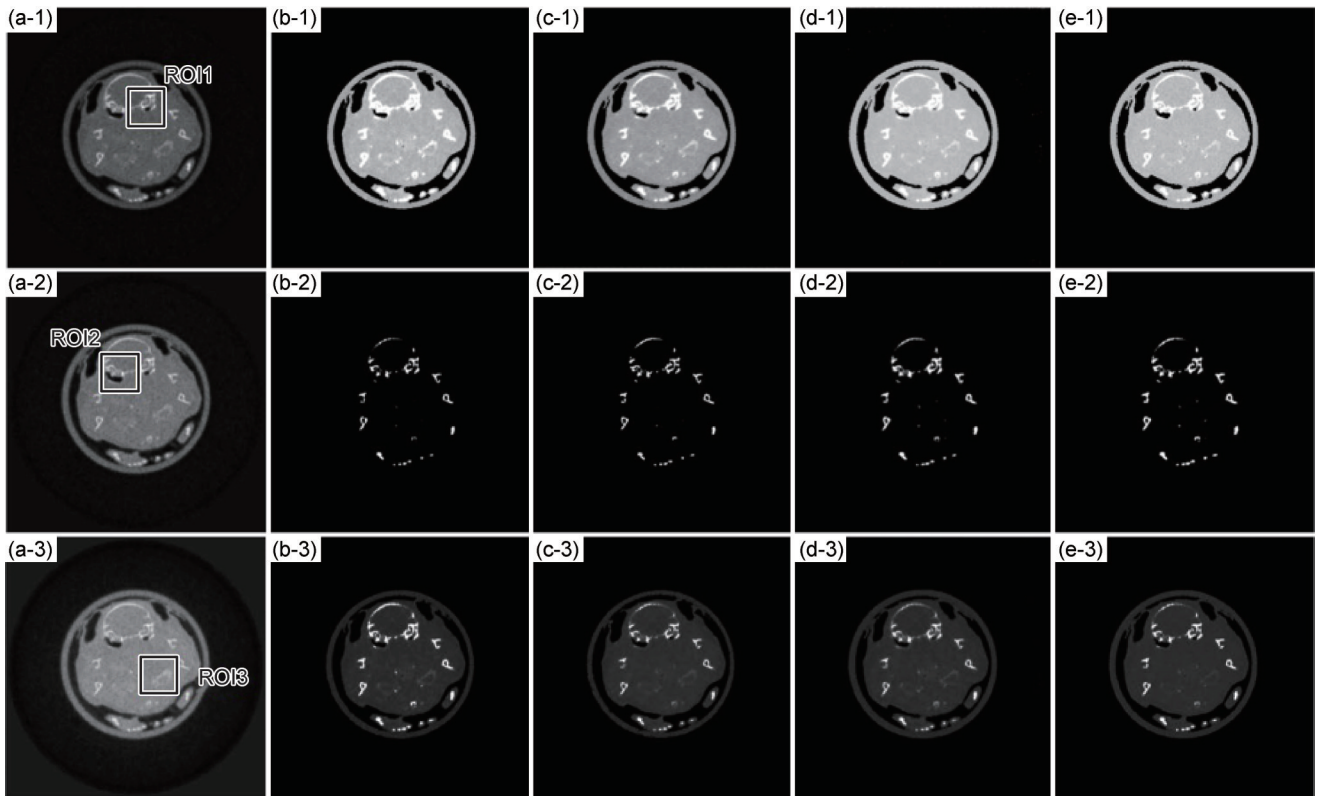


图11 水(1)、钙(2)和碘(3)的不同材料分解算法结果对比图

(a)重构图像;(b)FC-DenseNet^[27];(c)U-net^[84];(d)Inception-Net^[96];(e)GECCU-net^[88]

Fig.11 Comparison of the results of different material decomposition algorithms for water(1), calcium(2), and iodine(3)

(a)reconstructed images;(b)FC-DenseNet^[27];(c)U-net^[84];(d)Inception-Net^[96];(e)GECCU-net^[88]

参考文献

- [1] 戚俊成,刘宾,陈荣昌,等.X射线光场成像技术研究[J].物理学报,2019,68(2):96-101.
QI J C, LIU B, CHEN R C, et al. Research on X-ray light field imaging technology [J]. Acta Physica Sinica, 2019, 68 (2) : 96-101.
- [2] 詹美娜,倪松,余海军,等.大直径回转体零部件壳体局部加速器CT检测[J].光学学报,2024,44(22):139-151.
ZHAN M N, NI S, YU H J, et al. Local accelerator CT inspection of large-diameter rotating part shells [J]. Acta Optica Sinica, 2024, 44(22): 139-151.
- [3] WILLEMINK M J, PERSSON M, POURMORTEZA A, et al. Photon-counting CT: technical principles and clinical prospects [J]. Radiology, 2018, 289(2): 293-312.
- [4] DAOUD B, CAZEJUST J, TAVOLARO S, et al. Could spectral CT have a potential benefit in coronavirus disease (COVID-19)? [J]. American Journal of Roentgenology, 2021, 216 (2) : 349-354.
- [5] AGOSTINI A, FLORIDI C, BORGHERESI A, et al. Proposal of a low-dose, long-pitch, dual-source chest CT protocol on third-generation dual-source CT using a tin filter for spectral shaping at 100 kVp for coronavirus disease 2019 (COVID-19) patients: a feasibility study [J]. Radiologia Medica, 2020, 125(4): 365-373.
- [6] BRANDELIK S C, SKORNITZKE S, MOKRY T, et al. Quantitative and qualitative assessment of plasma cell dyscrasias in dual-layer spectral CT [J]. European Radiology, 2021, 31(10): 7664-7673.
- [7] SIMSIR B D, DANSE E, COCHE E. Benefit of dual-layer spectral CT in emergency imaging of different organ systems [J]. Clinical Radiology, 2020, 75(12): 886-902.
- [8] 杨富强,杨瑶,李志翔,等.X射线工业CT成像过程复杂伪影抑制方法综述[J].自动化学报,2023,49(4):687-704.
YANG F Q, YANG Y, LI Z X, et al. Overview of complex artifact suppression methods in X-ray industrial CT imaging process [J]. Acta Automatica Sinica, 2023, 49(4): 687-704.
- [9] 杨亚飞,张才鑫,陈华,等.基于光子计数能谱CT的含能材料等效原子序数测量方法[J].光谱学与光谱分析,2022,42(5):1400-1406.
YANG Y F, ZHANG C X, CHEN H, et al. Measurement method of equivalent atomic number for energetic materials based on photon-counting energy spectrum CT [J]. Spectroscopy and Spectral Analysis, 2022, 42(5): 1400-1406.
- [10] 李毅红,屈赵燕,赵晓杰,等.基于材料组分先验的X射线多能投影盲分离算法[J].光学学报,2021,41(23):85-94.
LI Y H, QU Z Y, ZHAO X J, et al. Blind separation algorithm for X-ray multi-energy projections based on material composition priors [J]. Acta Optica Sinica, 2021, 41(23): 85-94.
- [11] 王玮,郭恩宇,王同敏.铝基复合材料半固态压缩变形组织演化同步辐射原位CT研究[J].材料工程,2021,49(4):95-101.

- WANG W, GUO E Y, WANG T M. *In-situ* synchrotron radiation CT study on microstructural evolution of aluminum matrix composites during semi-solid compression deformation [J]. Journal of Materials Engineering, 2021, 49(4): 95-101.
- [12] 李保磊, 李斌, 张萍宇, 等. 高密度金属包装液体的双能 CT 检测方法[J]. 原子能科学技术, 2018, 52(4): 744-749.
- LI B L, LI B, ZHANG P Y, et al. Dual-energy CT detection method for high-density metal-packaged liquids [J]. Atomic Energy Science and Technology, 2018, 52(4): 744-749.
- [13] 皮真真, 余海军, 李雷, 等. 一种三源摆动螺旋安检 CT 成像方法研究[J]. 光学学报, 2021, 41(16): 93-102.
- PI Z Z, YU H J, LI L, et al. Research on a three-source swing helical security inspection CT imaging method [J]. Acta Optica Sinica, 2021, 41(16): 93-102.
- [14] 孔霞, 潘晋孝, 赵晓杰, 等. 层间约束下三维块匹配的双能 CT 多成分分解[J]. 光谱学与光谱分析, 2023, 43(3): 774-780.
- KONG X, PAN J X, ZHAO X J, et al. Multi-component decomposition in dual-energy CT based on three-dimensional block matching with interlayer constraints [J]. Spectroscopy and Spectral Analysis, 2023, 43(3): 774-780.
- [15] ALVAREZ R E, MACOVSKI A. Energy-selective reconstructions in X-ray computerized tomography [J]. Physics in Medicine and Biology, 1976, 21(5): 733-744.
- [16] 邸云霞, 孔慧华, 牛晓伟. 基于主成分分析的多能谱 CT 图像分析方法研究[J]. CT 理论与应用研究, 2022, 31(6): 749-760.
- DI Y X, KONG H H, NIU X W. Research on multi-energy spectrum CT image analysis method based on principal component analysis [J]. CT Theory and Applications, 2022, 31(6): 749-760.
- [17] ZHANG G, CHENG J, ZHANG L, et al. A practical reconstruction method for dual energy computed tomography [J]. Journal of X-ray Science and Technology, 2008, 16(2): 67-88.
- [18] BALLABRIGA R, ALOZY J, CAMPBELL M, et al. The Medipix3RX: a high resolution, zero dead-time pixel detector readout chip allowing spectroscopic imaging [J]. Journal of Instrumentation, 2013, 8: C02016.
- [19] 降俊汝, 余海军, 龚长城, 等. 基于双能 CT 图像域的 DL-RTV 多材料分解研究[J]. 光学学报, 2020, 40(21): 93-104.
- JIANG J R, YU H J, GONG C C, et al. Research on DL-RTV multi-material decomposition based on dual-energy CT image domain [J]. Acta Optica Sinica, 2020, 40(21): 93-104.
- [20] LI Z, RAVISHANKAR S, LONG Y, et al. Learned mixed material models for efficient clustering based dual-energy CT image decomposition [C] // 2018 IEEE Global Conference on Signal and Information Processing (GlobalSIP). Anaheim, CA: IEEE, 2018: 529-533.
- [21] HARMS J, WANG T H, PETRONGOLO M, et al. Noise suppression for dual-energy CT *via* penalized weighted least-square optimization with similarity-based regularization [J]. Medical Physics, 2016, 43(5): 2676-2686.
- [22] 周正东, 章栩苓, 辛润超, 等. 基于 MAP-EM 算法的双能 CT 直接迭代基材料分解方法[J]. 东南大学学报(自然科学版), 2020, 50(5): 935-941.
- ZHOU Z D, ZHANG X L, XIN R C, et al. Direct iterative basis material decomposition method for dual-energy CT based on MAP-EM algorithm [J]. Journal of Southeast University (Natural Science Edition), 2020, 50(5): 935-941.
- [23] LI Z, RAVISHANKAR S, LONG Y, et al. Dect-multra: dual-energy CT image decomposition with learned mixed material models and efficient clustering [J]. IEEE transactions on Medical Imaging, 2019, 39(4): 1223-1234.
- [24] ZHAO Y, ZHAO X, ZHANG P. An extended algebraic reconstruction technique (E-ART) for dual spectral CT [J]. IEEE Transactions on Medical Imaging, 2014, 34(3): 761-768.
- [25] LI Z, LONG Y, CHUN I Y. An improved iterative neural network for high-quality image-domain material decomposition in dual-energy CT [J]. Medical Physics, 2023, 50(4): 2195-2211.
- [26] DI T V, BROMBAL L, BRUN F. Multi-material spectral photon-counting micro-CT with minimum residual decomposition and self-supervised deep denoising [J]. Optics Express, 2022, 30(24): 42995-43011.
- [27] WU X C, HE P, LONG X D, et al. Multi-material decomposition of spectral CT images *via* fully convolutional densenets [J]. Journal of X-ray Science and Technology, 2019, 27(3): 461-471.
- [28] LELL M M, KACHELRIESS M. Recent and upcoming technological developments in computed tomography: high speed, low dose, deep learning, multienergy [J]. Investigative Radiology, 2020, 55(1): 8-19.
- [29] JOHNSON T R C, KRAUSS B, SEDLMAIR M, et al. Material differentiation by dual energy CT: initial experience [J]. European Radiology, 2007, 17(6): 1510-1517.
- [30] KARCAALTINCABA M, AKTAS A. Dual-energy CT revisited with multidetector CT: review of principles and clinical applications [J]. Diagnostic and Interventional Radiology, 2011, 17(3): 181-194.
- [31] PANETTA D. Advances in X-ray detectors for clinical and pre-clinical computed tomography [J]. Nuclear Instruments and Methods in Physics Research Section A: Accelerators, Spectrometers, Detectors and Associated Equipment, 2016, 809: 2-12.
- [32] SCHUMACHER D, SHARMA R, GRAGER J C, et al. Scatter and beam hardening reduction in industrial computed tomography using photon counting detectors [J]. Measurement Science and Technology, 2018, 29(7): 075101.
- [33] CHEN B, ZHANG Z, SIDKY E Y, et al. Image reconstruction and scan configurations enabled by optimization-based algorithms in multispectral CT [J]. Physics in Medicine and Biology, 2017, 62(22): 8763-8793.
- [34] LI L, CHEN Z, WANG G, et al. A tensor PRISM algorithm for multi-energy CT reconstruction and comparative studies [J]. Journal of X-ray Science and Technology, 2014, 22(2): 147-163.
- [35] ROESSL E, PROKSA R. K-edge imaging in X-ray computed tomography using multi-bin photon counting detectors [J]. Physics in Medicine and Biology, 2007, 52(15): 4679-4696.
- [36] MEERT C A, MACDONALD A T, JINIA A J, et al. Photon-neutron detection in active interrogation scenarios using small or-

- ganic scintillators [J]. IEEE Transactions on Nuclear Science, 2022, 69(6): 1397-1402.
- [37] BALLABRIGA R, CAMPBELL M, HEIJNE E, et al. Medipix3: a 64 k pixel detector readout chip working in single photon counting mode with improved spectrometric performance [J]. Nuclear Instruments and Methods in Physics Research Section A: Accelerators, Spectrometers, Detectors and Associated Equipment, 2011, 633(1): S15-S18.
- [38] HENRICH B, BERGAMASCHI A, BROENNIMANN C, et al. PILATUS: a single photon counting pixel detector for X-ray applications [J]. Nuclear Instruments and Methods in Physics Research Section A: Accelerators, Spectrometers, Detectors and Associated Equipment, 2009, 607(1): 247-249.
- [39] TAGUCHI K, IWANCZYK J S. Vision 20/20: single photon counting X-ray detectors in medical imaging [J]. Medical Physics, 2013, 40(10): 100901.
- [40] KALENDER W A, PERMAN W H, VETTER J R, et al. Evaluation of a prototype dual-energy computed tomographic apparatus. I. phantom studies [J]. Medical Physics, 1986, 13(3): 334-339.
- [41] SCHLOMKA J P, ROESSL E, DORSCHIED R, et al. Experimental feasibility of multi-energy photon-counting K-edge imaging in pre-clinical computed tomography [J]. Physics in Medicine and Biology, 2008, 53(15): 4031-4047.
- [42] SCHIRRA C O, ROESSL E, KOEHLER T, et al. Statistical reconstruction of material decomposed data in spectral CT [J]. IEEE transactions on Medical Imaging, 2013, 32(7): 1249-1257.
- [43] LIU X, YU L, PRIMAK A N, et al. Quantitative imaging of element composition and mass fraction using dual-energy CT: Three-material decomposition [J]. Medical Physics, 2009, 36(5): 1602-1609.
- [44] 李保磊, 张耀军. 基于投影匹配的X射线双能计算机层析成像投影分解算法 [J]. 光学学报, 2011, 31(3): 82-87.
- LI B L, ZHANG Y J. Projection decomposition algorithm for X-ray dual-energy computed tomography based on projection matching [J]. Acta Optica Sinica, 2011, 31(3): 82-87.
- [45] ZHANG W, ZHAO S, PAN H, et al. A locally weighted linear regression look-up table-based iterative reconstruction method for dual spectral CT [J]. IEEE Transactions on Biomedical Engineering, 2023, 70(11): 3028-3039.
- [46] DUCROS N, ABASCAL J F P J, SIXOU B, et al. Regularization of nonlinear decomposition of spectral X-ray projection images [J]. Medical Physics, 2017, 44(9): E174-E187.
- [47] ZHAO X, LI Y, HAN Y, et al. Statistical iterative spectral CT imaging method based on blind separation of polychromatic projections [J]. Optics Express, 2022, 30(11): 18219-18237.
- [48] CONG W X, DE M B, WANG G. Projection decomposition *via* univariate optimization for dual-energy CT [J]. Journal of X-Ray Science and Technology, 2022, 30(4): 725-736.
- [49] LU C, HAN Z Y, ZOU J. Projection domain decomposition denoising algorithm based on low rank and similarity-based regularization [J]. Journal of X-Ray Science and Technology, 2024, 32(3): 549-568.
- [50] WANG B P, ZHANG L X, FAN J L, et al. New filtered back-projection algorithm [J]. Computer Engineering and Application, 2009, 32(45): 16-18.
- [51] ZHANG Y B, MOU X Q, WANG G, et al. Tensor-based dictionary learning for spectral CT reconstruction [J]. IEEE Transactions on Medical Imaging, 2017, 36(1): 142-154.
- [52] KONG H H, LEI X X, LEI L, et al. Spectral CT reconstruction based on PICCS and dictionary learning [J]. IEEE Access, 2020, 8: 133367-133376.
- [53] XUE Y, RUAN R, HU X, et al. Statistical image-domain multi-material decomposition for dual-energy CT [J]. Medical Physics, 2017, 44(3): 886-901.
- [54] HAO J, KANG K, ZHANG L, et al. A novel image optimization method for dual-energy computed tomography [J]. Nuclear Instruments & Methods in Physics Research Section A-Accelerators Spectrometers Detectors and Associated Equipment, 2013, 722: 34-42.
- [55] JIANG Y, XUE Y, LYU Q, et al. Noise suppression in image-domain multi-material decomposition for dual-energy CT [J]. IEEE Transactions on Biomedical Engineering, 2019, 67(2): 523-535.
- [56] 李思宇, 张欣睿, 蔡爱龙, 等. 基于能谱CT的青铜器等效原子序数与密度估计方法 [J]. 光学学报, 2024, 44(4): 176-182.
- LI S Y, ZHANG X R, CAI A L, et al. Method for estimating equivalent atomic number and density of bronze ware based on spectral CT [J]. Acta Optica Sinica, 2024, 44(4): 176-182.
- [57] JUMANAZAROV D, ALIMOVA A, ABDIKARIMOV A, et al. Material classification using basis material decomposition from spectral X-ray CT [J]. Nuclear Instruments & Methods in Physics Research Section A-Accelerators Spectrometers Detectors and Associated Equipment, 2023, 1056: 168637.
- [58] NIU T, DONG X, PETRONGOLO M, et al. Iterative image-domain decomposition for dual-energy CT [J]. Medical Physics, 2014, 41(6): 27.
- [59] MENDONCA P R S, LAMB P, SAHANI D V. A flexible method for multi-material decomposition of dual-energy CT images [J]. IEEE Transactions on Medical Imaging, 2013, 33(1): 99-116.
- [60] ZHOU Z D, ZHANG X L, XIN R C, et al. Direct iterative basis image reconstruction based on MAP-EM algorithm for spectral CT [J]. Journal of Nondestructive Evaluation, 2021, 40(1): 5.
- [61] WU W, YU H, CHEN P, et al. Dictionary learning based image-domain material decomposition for spectral CT [J]. Physics in Medicine and Biology, 2020, 65(24): 245006.
- [62] XIE B, SU T, KAFTANDJIAN V, et al. Material decomposition in X-ray spectral CT using multiple constraints in image domain [J]. Journal of Nondestructive Evaluation, 2019, 38(1): 16.
- [63] ZHANG T, YU H, XI Y, et al. Spectral CT image-domain material decomposition *via* sparsity residual prior and dictionary learning [J]. IEEE Transactions on Instrumentation and Measurement, 2023, 72: 1-13.
- [64] HU J, ZHAO X, WANG F. An extended simultaneous algebraic

- reconstruction technique (E-SART) for X-ray dual spectral computed tomography[J]. *Scanning*, 2016, 38(6): 599-611.
- [65] ZHANG W, ZHAO S, PAN H, et al. An iterative reconstruction method based on monochromatic images for dual energy CT [J]. *Medical Physics*, 2021, 48(10): 6437-6452.
- [66] ZHAO S, PAN H, ZHANG W, et al. An oblique projection modification technique (OPMT) for fast multispectral CT reconstruction [J]. *Physics in Medicine and Biology*, 2021, 66(6): 065003.
- [67] PAN H, ZHAO S, ZHANG W, et al. Fast iterative reconstruction for multi-spectral CT by a Schmidt orthogonal modification algorithm (SOMA) [J]. *Inverse Problems*, 2023, 39(8): 085001.
- [68] YU X, CAI A, LIANG N, et al. Volume conservation constrained multi-material reconstruction for inconsistent spectral CT Imaging[J]. *IEEE Access*, 2024, 12: 58128-58142.
- [69] CAI C, RODET T, LEGOUPIL S, et al. A full-spectral Bayesian reconstruction approach based on the material decomposition model applied in dual-energy computed tomography[J]. *Medical Physics*, 2013, 40(11): 111916.
- [70] LONG Y, FESSLER J A. Multi-material decomposition using statistical image reconstruction for spectral CT [J]. *IEEE Transactions on Medical Imaging*, 2014, 33(8): 1614-1626.
- [71] BARBER R F, SIDKY E Y, SCHMIDT T G, et al. An algorithm for constrained one-step inversion of spectral CT data [J]. *Physics in Medicine and Biology*, 2016, 61(10): 3784-3818.
- [72] BARBER R F, SIDKY E Y. Convergence for nonconvex ADMM, with applications to CT imaging[J]. *Journal of Machine Learning Research*, 2024, 25: 38.
- [73] SCHMIDT T G, SAMMUT B A, BARBER R F, et al. Addressing CT metal artifacts using photon-counting detectors and one-step spectral CT image reconstruction [J]. *Medical Physics*, 2022, 49(5): 3021-3040.
- [74] ZHANG W, CAI A, ZHENG Z, et al. A Direct material reconstruction method for DECT based on total variation and BM3D frame[J]. *IEEE Access*, 2019, 7: 138579-138592.
- [75] YU X, CAI A, LIANG N, et al. Direct multi-material reconstruction *via* iterative proximal adaptive descent for spectral CT Imaging[J]. *Bioengineering-Basel*, 2023, 10(4): 470.
- [76] YANG Z J, ZENG L, YU W, et al. Anisotropic sparse transformation for spectral CT image reconstruction [J]. *IET Image Processing*, 2024, 18(13): 3916-3934.
- [77] ZHANG K, ZUO W M, CHEN Y J, et al. Beyond a Gaussian denoiser: residual learning of deep CNN for image denoising [J]. *IEEE Transactions on Image Processing*, 2017, 26(7): 3142-3155.
- [78] 邸拴虎, 杨文瀚, 廖苗, 等. 基于 RA-Unet 的 CT 图像肝脏肿瘤分割 [J]. *仪器仪表学报*, 2022, 43(8): 65-72.
- DI S H, YANG W H, LIAO M, et al. Liver tumor segmentation in CT images based on RA-Unet [J]. *Chinese Journal of Scientific Instrument*, 2022, 43(8): 65-72.
- [79] RANI K, KUMAR S. Hyperspectral image classification using a new deep learning model based on pseudo-3D block and depth separable 2D-3D convolution [J]. *Engineering Applications of Artificial Intelligence*, 2024, 130: 107738.
- [80] SHI W, ZHU Z, ZHANG K, et al. SMIFormer: learning spatial feature representation for 3D object detection from 4D imaging radar *via* multi-view interactive transformers [J]. *Sensors*, 2023, 23(23): 9429.
- [81] BERA S, BISWAS P K. Noise conscious training of non local neural network powered by self attentive spectral normalized Markovian patch GAN for low dose CT denoising [J]. *IEEE Transactions on Medical Imaging*, 2021, 40(12): 3663-3673.
- [82] 马燕, 余海军, 钟发生, 等. 基于残差编解码网络的 CT 图像金属伪影校正 [J]. *仪器仪表学报*, 2020, 41(8): 160-169.
- MA Y, YU H J, ZHONG F S, et al. Metal artifact correction in CT images based on residual encoder-decoder network [J]. *Chinese Journal of Scientific Instrument*, 2020, 41(8): 160-169.
- [83] CHEN Z, LI L. Robust multimaterial decomposition of spectral CT using convolutional neural networks [J]. *Optical Engineering*, 2019, 58(1): 013104.
- [84] CLARK D P, HOLBROOK M, BADEA C T. Multi-energy CT decomposition using convolutional neural networks [C] // *Medical Imaging 2018: Physics of Medical Imaging*. Houston, TX: SPIE, 2018: 415-423.
- [85] XU Y, YAN B, ZHANG J, et al. Image decomposition algorithm for dual-energy computed tomography *via* fully convolutional network [J]. *Computational and Mathematical Methods in Medicine*, 2018, 2018: 2527516.
- [86] ZHANG W, ZHANG H, WANG L, et al. Image domain dual material decomposition for dual-energy CT using butterfly network [J]. *Medical Physics*, 2019, 46(5): 2037-2051.
- [87] SU T, SUN X, YANG J, et al. DIRECT-Net: A unified mutual-domain material decomposition network for quantitative dual-energy CT imaging [J]. *Medical Physics*, 2022, 49(2): 917-934.
- [88] SHI Z F, KONG F N, CHENG M, et al. Multi-energy CT material decomposition using graph model improved CNN [J]. *Medical & Biological Engineering & Computing*, 2024, 62(4): 1213-1228.
- [89] GOODFELLOW I, POUGETT A J, MIRZA M, et al. Generative adversarial nets [J]. *Advances in Neural Information Processing Systems*, 2014, 27: 2672-2680.
- [90] GENG M, TIAN Z, JIANG Z, et al. PMS-GAN: parallel multi-stream generative adversarial network for multi-material decomposition in spectral computed tomography [J]. *IEEE Transactions on Medical Imaging*, 2020, 40(2): 571-584.
- [91] SHI Z, LI H, CAO Q, et al. A material decomposition method for dual-energy CT *via* dual interactive Wasserstein generative adversarial networks [J]. *Medical Physics*, 2021, 48(6): 2891-2905.
- [92] GUO X, HE P, LV X, et al. Material decomposition of spectral CT images *via* attention-based global convolutional generative adversarial network [J]. *Nuclear Science and Techniques*, 2023, 34(3): 45.
- [93] LYU T, ZHAO W, ZHU Y, et al. Estimating dual-energy CT

- imaging from single-energy CT data with material decomposition convolutional neural network[J]. *Medical Image Analysis*, 2021, 70: 102001.
- [94] KOIKE Y, OHIRA S, YAMAMOTO Y, et al. Artificial intelligence-based image-domain material decomposition in single-energy computed tomography for head and neck cancer[J]. *International Journal of Computer Assisted Radiology and Surgery*, 2024, 19(3): 541-551.
- [95] WANG G S, LIU Z, HUANG Z Y, et al. Improved GAN: using a transformer module generator approach for material decomposition [J]. *Computers in Biology and Medicine*, 2022, 149: 105952.
- [96] GONG H, TAO S Z, RAJENDRAN K, et al. Deep-learning-based direct inversion for material decomposition [J]. *Medical Physics*, 2020, 47(12): 6294-6309.
- [97] ABASCAL J F P J, DUCROS N, PRONINA V, et al. Material decomposition in spectral CT using deep learning: a Sim2Real transfer approach[J]. *IEEE Access*, 2021, 9: 25632-25647.
- [98] SHIN H C, ROTH H R, GAO M, et al. Deep convolutional neural networks for computer-aided detection: CNN architectures, dataset characteristics and transfer learning[J]. *IEEE transactions on Medical Imaging*, 2016, 35(5): 1285-1298.
-
- 基金项目:**中国航空发动机集团产学研合作项目(HFZL2022CXY024);浙江省“尖兵领雁+X”研发攻关计划(2024C01249(SD2));西北工业大学硕士研究生实践创新能力培育基金项目(PF2025051)
- 收稿日期:**2025-03-04;**录用日期:**2025-04-14
- 通讯作者:**黄魁东(1978—),男,副教授,博士,主要研究方向为锥束CT理论和应用、计算机图形图像处理,联系地址:陕西省西安市碑林区友谊西路127号西北工业大学友谊校区机电学院(710072),E-mail: kdhuang@nwpu.edu.cn
- (本文责编:张宝玲)